Fault tolerance analysis of a hexarotor with reconfigurable tilted rotors

Claudio Pose, Juan Giribet and Ignacio Mas

***Abstract*— Tilted rotors in multirotor vehicles have shown to be useful for different practical reasons. For instance, increasing yaw maneuverability or enabling full position and attitude control of hexarotor vehicles. It has also been proven that a hexagon-shaped multirotor is capable of complete attitude and altitude control under failures of one of its rotors. However, when a rotor fails, the torque that can be reached in the worst-case direction decreases considerably.**

This work proposes to actively change the tilt angle of the rotors when a failure occurs. This rotor reconfiguration increases the maximum torque that can be achieved in the most stressful direction, reducing maneuverability limitations. Experimental validations are shown, where the proposed reconfigurable tilted rotor is used in order to control a hexarotor vehicle when a failure appears mid-flight. The impact of the delay in the reconfiguration when a failure occurs is also addressed.

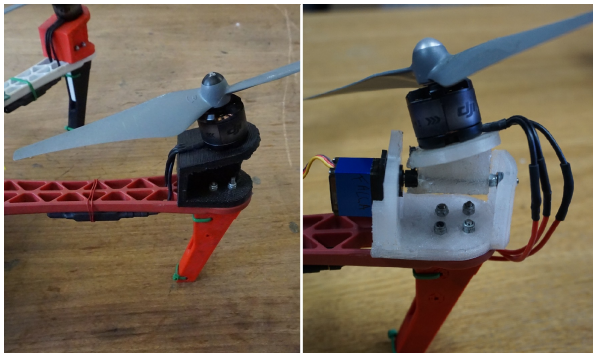

Fig. 1. Proposed reconfigurable hexarotor design for fault tolerance against full rotor failures. Rotor tilted inwards (left), and reconfigurable rotor with servo operation (right).

I. Introduction

Multirotor aerial vehicles have become very popular in recent years, due to the increased availability of the electronic systems needed to fly them, as well as the reduction of their cost and weight. Simplicity and cost-effectiveness have turned out to be very appealing and, as a consequence, an increasing number of applications have risen in many fields, such as agriculture, surveillance, and photography, among others. Fault tolerance has been addressed in the literature as a matter of high importance, in particular for multirotor vehicles, see for instance [1], [2], [3], [4], [5], [6], and references therein.

In particular, in [7] the capability of compensating for a rotor failure without losing the ability to exert torques in all directions–and therefore keeping full attitude control in case of failure–was studied. To achieve this, at least six rotors are needed, and they must be tilted with respect to the vertical axis of the vehicle. The proposed solution in [7] was to tilt the rotors (or arms) of the hexarotor inwards. Experimental results for the proposed solution can be found in [8], where the vehicle takes off, performs different maneuvers, and lands successfully with one motor in total failure, maintaining full attitude and altitude control. While the system proved to work correctly, there was a direction that, when exerted torque in, performed noticeably worse with respect to the rest. In [9], a detailed analysis is made with respect to the optimal orientations of the rotors in a hexarotor, in order to achieve full tolerant attitude control. But, even in this case, in some real applications, when a motor fails, the maximum torque achievable in some directions may be too small, with the consequent degradation of vehicle maneuverability.

Reconfigurable-rotor vehicles have been proposed for improving vehicle maneuverability, see for instance [10], [11], [12], and reference therein. In [13], it was shown that, if the rotors have the ability to change the direction of rotation, fault-tolerance is possible with a non-tilted hexarotor vehicle. However, unless reconfigurable propellers are used, thrust in the opposite direction is exerted if the direction of rotation is reversed. This limitation could be solved, but with a more complex mechanical system.

In this work, the addition of reconfigurable rotors is proposed in order to tilt the rotors when a total failure occurs in one of the remaining rotors. This allows to improve the maximum achievable torque in the worst-case direction. Since the addition of mechanisms for rotor reconfiguration increases weight, cost, and number of mechanical parts of the vehicle (increasing the probability of a failure), it is desirable to minimize the number of added components.

The proposed vehicle is a hexarotor with inward-tilted rotors (guaranteeing full attitude control, even if one rotor fails), where two of them have the capability of tilting sideways (see Fig. 1), improving the maximum achievable torque in the worst-case direction. An experimental flight is shown, where the vehicle recovers from a total failure that appears mid-flight. Additionally, several experiments considering different delays between failure and reconfiguration to account for detection times are presented.

II. Tilted-rotor vehicle model

When dealing with total rotor failures in hexarotors, it has been proven that a standard hexarotor configuration (one

Claudio Pose, Juan Giribet and Ignacio Mas are with LAR-GPSIC - Facultad de Ingeniería, Universidad de Buenos Aires, Buenos Aires, Argentina. [cldpose, jgiribet, imas]@fi.uba.ar

Juan Giribet is with the Instituto Argentino de Matemática - CONICET, Buenos Aires, Argentina.

Ignacio Mas is with CONICET - Instituto Tecnológico de Buenos Aires, Buenos Aires, Argentina.

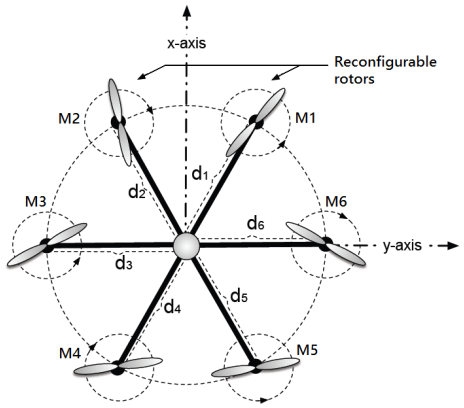

Fig. 2. Top view of the proposed reconfigurable hexarotor.

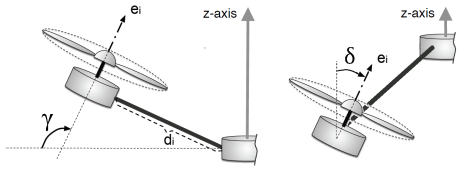

Fig. 3. Side view of the proposed reconfigurable hexarotor. γ denotes the inward/outward tilt and δ the side tilt.

with the rotors spaced evenly in a plane, pointing upwards, with alternated spinning direction, as in Fig. 2) is not fault tolerant in the event of a failure of this type, in the sense of maintaining control over its four degrees of freedom (rotation around its three axis, and vertical speed). One degree of freedom will be lost, being generally the yaw axis the one chosen to lose control of, as it allows the possibility to land the vehicle safely. From this point on, fault tolerance will be meant in the sense that the system maintains complete altitude and attitude control.

Suppose a standard hexarotor configuration with $\gamma = 90^o$ (see Fig. 3), which, while in hovering mode, suffers a total loss of rotor number 3 (M3), a counter-clockwise (CCW) rotating motor. Then, this rotor no longer generates thrust to produce torque on the x-axis, and neither does it generate torque on the z-axis due to the spinning propeller. To compensate for the failure, the only feasible solution to exert zero torque is that in which the opposite rotor, which generates exactly the opposite torque, exerts zero force. In this case, the system is not fault tolerant, as there will exist a torque $\mathbf{q}_w = (M_x, M_y, M_z)$ (worst case direction torque) that will require a negative speed from M6 (see [7]), which cannot be achieved. The solution using the inward-tilted rotors with $\gamma > 90^o$, allows M6 to hold the hovering state with a small positive speed, which in turn allows the vehicle to exert torque in the direction $\mathbf{q}_w$. However, the maximum achievable magnitude of this torque is small, as the maneuver is limited by the saturation of M6. Rotation in the yaw axis is the most stressful maneuver, as it requires higher speed variations from the motors with respect to similar maneuvers in pitch or roll.

A better solution, as it was shown in [9], is to tilt the rotors an angle δ around its arm's axis. However, in some practical situations the improvement is not enough to have good vehicle maneuverability under failure. The reason is that, in both vehicles (with $\delta = 0$ and $\delta > 0$), all rotors produce the same torque in yaw if driven at the same speed. In consequence, when one of them fails, there appears a large torque in that axis that has to be compensated. In what follows, angle δ_i is defined as the rotation of rotor i around its arm's axis, as shown in Fig. 3.

As the main issue in case of a failure appears to be the yaw control, suppose now an inward-tilted rotor, with $\gamma > 90^o$, in which M1 has a servo to control a variable angle δ_1, while the rest of the motors remain with a fixed $\delta_i = 0,\ i = 2, ..., 6$. Qualitatively, in the case of a failure in a CCW motor (same rotating direction as M1), a tilt angle $\delta_1 > 0$ could be selected in order to increase the torque that M1 is already exerting in yaw, to compensate for the loss of torque in that axis. On the other hand, if a CW motor fails, $\delta_1 < 0$ may be used to reduce or reverse the torque in yaw produced by M1. This intuitive concept, can be formally analyzed as follows.

In a normal state of operation, when all motors are working properly, with $\delta_1 = 0$, each one produces a force $f_i \in [0, F_M]$. In practice, a motor is commanded through a Pulse Width Modulated (PWM) signal u_i, which goes from 0 to 100%. Near the nominal operating point, a linear relation between the PWM signal and the exerted force is assumed, with $f_i = k_f u_i$. It is also considered that each motor exerts a torque on its spinning axis, $m_i = (-1)^i k_t u_i$. The k_f and k_t, constants are usually established experimentally. There exists a desired torque and vertical force $\mathbf{q} = (M_x, M_y, M_z, F_z)$. A relationship between these magnitudes is given by the following equation:

$$\mathbf{q} = \begin{bmatrix} M_x \\ M_y \\ M_z \\ F_z \end{bmatrix} = A(\gamma, \delta_1) \cdot f, \qquad \text{with} \qquad \mathbf{f} = \begin{bmatrix} f_1 \\ \vdots \\ f_6 \end{bmatrix}. \quad (1)$$

Force-torque matrix $A = A(\gamma, \delta_1) \in \mathbb{R}^{4\times 6}$ is given by:

$$A = \begin{bmatrix} \tilde{k}_t c\gamma[& -1 & \frac{\alpha+1}{2\alpha} & \frac{\alpha+1}{2\alpha} & -1 & \frac{\alpha-1}{2\alpha} & \frac{\alpha-1}{2\alpha}] \\ \tilde{k}_t\sqrt{3}c\gamma[& a_{21} & \frac{3\alpha-1}{6\alpha} & -\frac{3\alpha-1}{6\alpha} & \frac{1}{3\alpha} & \frac{3\alpha+1}{6\alpha} & -\frac{3\alpha+1}{6\alpha}] \\ \tilde{k}_t s\gamma[& c\delta_1 & -1 & 1 & -1 & 1 & -1] \\ -s\gamma[& c\delta_1 & 1 & 1 & 1 & 1 & 1] \end{bmatrix}$$

$$a_{21} = -\frac{c\delta_1}{3\alpha} + \frac{k_t s\delta_1}{3\alpha l}, \text{ and } \alpha = \frac{\tilde{k}_t}{\sqrt{3}\ l \tan(\gamma)},$$

where $l = \|d_i\|$, the notation $s\varphi = \sin(\varphi)$ and $c\varphi = \cos(\varphi)$ is used, and $\tilde{k}_t = k_t/k_f$.

In the case of a total failure in a rotor i (from M2 to M6), the system may be modeled by replacing the $i-th$ column of the matrix A with zeros, which will be denoted as $A_i(\gamma, \delta_1)$.

The problem of finding a force set $f \geq 0$ to achieve the desired torque-force vector $\mathbf{q}$, usually is solved by using the Moore-Penrose pseudoinverse of A, denoted as $A^\dagger$, that yields the minimum energy solution:

$$\mathbf{f} = A^\dagger(\gamma, \delta_1)\mathbf{q}, \quad (2)$$

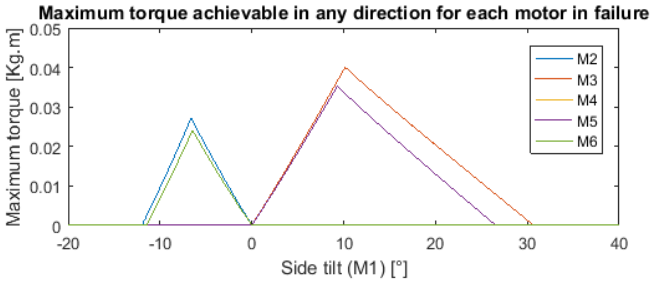

Fig. 4. Maximum torque achievable in *any* direction, with respect to the side-tilt angle of M1, for a failure in one of the motors from M2 to M6.

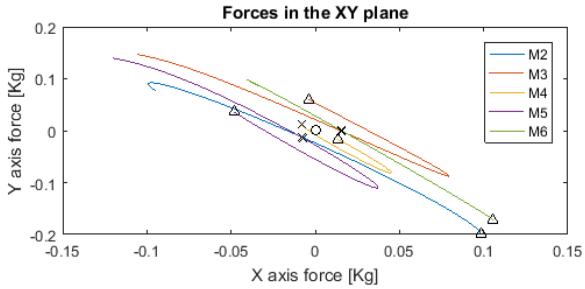

Fig. 5. Resulting forces in the *xy* plane (for different values of $\delta_1 \in [-20^o, 40^o]$), for a failure in rotors M2 to M6. The circle marks the (0,0) force, the crosses mark the force for $\delta_1 = 0^o$, and the triangles mark the force for $\delta_1 = -20^o$.

where $A^\dagger$ is replaced by $A_i^\dagger = A_i(\gamma, \delta_1)^\dagger$ in case of a failure in rotor i.

It remains to consider that a failure may also occur in M1, in which case changing δ_1 would have no effect on the system, resulting in the original inwards tilted vehicle. So, it will be required to add at least a second servo in another motor. The number of needed servos and the adequate location for them is discussed in the following section.

III. Proposed Rotors Configuration

To study the advantages and limitations of the proposed solution, a numerical study was carried out, considering that all motors are tilted inwards with $\gamma = 107^o$ (as it was used in [8]), and only M1 is tilted sideways an angle δ_1. The torque capabilities of the vehicle will be analyzed for a total failure in each of the remaining motors.

Suppose now that the vehicle is in a hovering state, at constant altitude (with a vertical force equal to its weight). Then, for each of the possible failures, there exists a direction $\mathbf{q}_w$ in which the torque that can be exerted is limited the most. In Fig. 4, the magnitude of $\mathbf{q}_w$ is shown, for a given range of the tilt angle δ_1 of M1, with each of the curves corresponding to a different motor in total failure.

The figure shows that, if a failure occurs in M3 or M5, the optimal δ_1 in order to maximize $\mathbf{q}_w$ is positive (approximately 10^o), i.e., M1 has to be tilted in such a way that the torque in yaw that it is already exerting is increased. This is due to M1, M3 and M5 being all of the CCW rotating type, so a lack of torque in yaw due to the loss of one of those motors is compensated by increasing the torque in yaw of a motor of the same spinning direction. For a failure in M2 or M6, the optimal δ_1 is negative (around -7^o), which means that M1 will be trying to reduce (or reverse) the torque it produces in yaw.

In case of a failure in M4, there is not a noticeable improvement in the maximum torque, for the range of δ_1 analyzed. This is because, when a failure occurs in one motor, the opposite one tends to work at a very low speed in order to keep the symmetry (in this case M1), which is the one that should be tilted to compensate the system.

The issue of a possible failure in M1 requires the addition of at least another servo. Two servos cannot be placed in opposite rotors, as a failure in a rotor with a servo would result in almost turning off the opposite one, being the case described above of a failure in M4. Additionally, observe that in the case described the vehicle performs better for failures in CCW spinning rotors (same direction as M1). Then, it is logical to place the second servo in a CW spinning rotor, which should be either M2 or M6.

Then, the proposed solution is that two contiguous, opposite-spinning rotors are configured to be tilted with a servo; for example, let them be M1 and M2. If one of the motors from M3 to M6 fails, the motor with the same spinning direction will be tilted with $\delta_i > 0$. If M1 or M2 fails, the other one will be tilted with $\delta_i < 0$, with a maximum torque lower than the previous case, but still much better than if it wasn't tilted at all. Something that can be noted is that the servos do not need to be continuously controlled once a failure occurs, as a fixed angle may be chosen for each possible failure (for example $\delta_{1,2} = 10^o$ and $\delta_{1,2} = -7^o$), in order to achieve a good performance.

When using M1 (or M2) with $\delta_1 \neq 0$, a part of the thrust force generated by the motor is projected onto the *xy* plane of the vehicle. The magnitude and direction of this force in hovering (zero pitch and roll), for $\delta_1 \in [-20^o, 40^o]$ is shown in Fig. 5. It can be noticed that a failure either in M3 or M5 produces similar results (but in different directions), as well as a failure in M2 or M6, due to the symmetry of the system. In practice, this force generates a noticeable drift in position over time, but can be easily compensated with the control system.

A comparison of the achievable torque sets is presented in Fig. 6 and Fig. 7, for vehicles with a total failure in M3. In Fig. 6, in red, the achievable torque space is shown for the inward-tilted hexacopter with $\gamma = 107^o$ and $\delta = 0^o$ for all motors. It can be observed that the origin (hovering mode), is very close to one of the faces of the polytope. The distance from the origin to the boundary of the set gives the magnitude of the worst case torque $\mathbf{q}_w$. In the same figure, in cyan, there is the torque map for the structure proposed in [9], but with $\gamma = 107^o$ and $\delta = 10^o$ for all motors. In this case, the total volume of the space is enlarged, but the magnitude $\mathbf{q}_w$ increases not that much as it would be expected for an acceptable vehicle behaviour. In Fig. 7, the same space is represented for the proposed solution, with $\gamma = 107^o$, $\delta_1 = 10^o$ and $\delta_i = 0^o$, $i = 2, ..., 6$. The volume

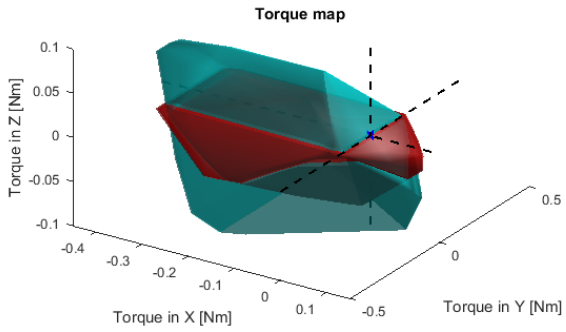

Fig. 6. Map of achievable torques space for an inward-tilted hexacopter with $\delta = 0$ (red) and with $\delta = 10^o$ (cyan) for all rotors, in case of a failure in M3

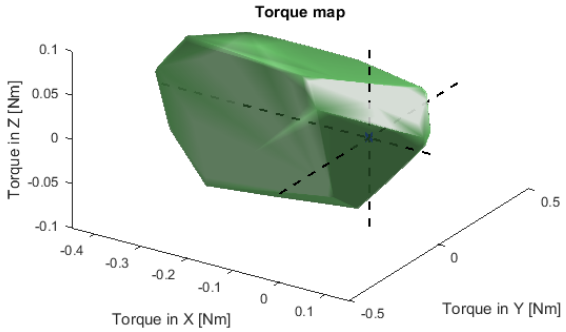

Fig. 7. Map of achievable torques space for an inward-tilted hexacopter with $\delta_1 = 10^o$ and $\delta_i = 0^o,\ i = 2, ..., 6$, in case of a failure in M3

of the torque space is bigger than in the first case and smaller that in the second case, but the distance from the origin to the boundary of the set is greatly increased, and also is the magnitude of $\mathbf{q}_w$.

The solution proposed in this work could be further improved by using a servo in each of the six rotors to control the tilting angle δ_i, which will naturally increase the overall mechanical complexity, but will also increase the weight of the vehicle. For a mid-range, $3Kg$ hexarotor with an average payload capacity of $0.5Kg$, with $1Kg$ thrust rotors, a robust small servo as [14] is required, which would weight around $40g$ considering all the pieces and wiring. This would mean an increase of $240g$ in the total weight, halving the available payload and also reducing the flight time.

IV. Simulation Results

To provide a numerical comparison of the in-flight performance between the inward-tilted vehicles with $\delta = 0^o$ and $\delta_1 = 10^o$, two simulations, carried out in MATLAB Simulink, are presented. The simulation model resembles the vehicles used in the experiments.

The simulations consist in two 40-seconds flights, with identical initial conditions, where the vehicles start in hovering state in a fixed point in space, $40m$ above the ground, with position control. A total failure in M3 exists from the beginning of the flight. The same perturbation profile that represents possible winds is applied to both vehicles, as shown in Fig. 8. The profile was randomly generated, and its

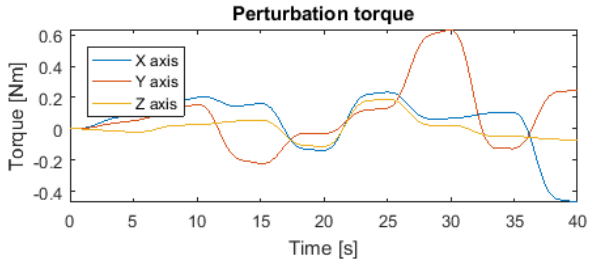

Fig. 8. Simulation results of perturbation torque exerted on each axis during a 40s time lapse.

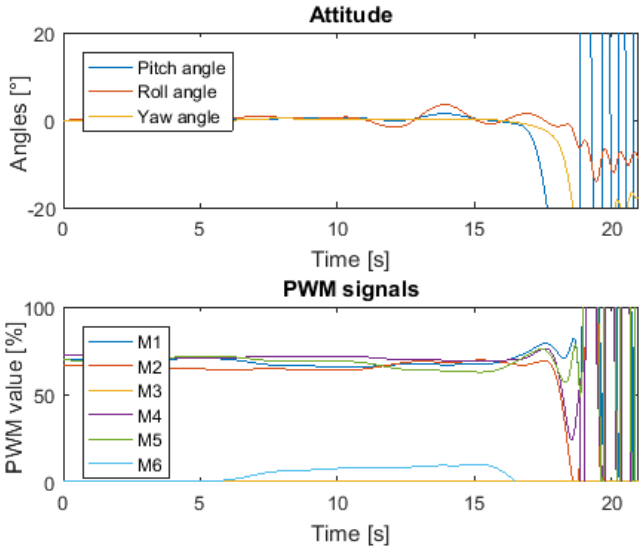

Fig. 9. Simulation results of attitude and PWM signals of the inward-tilted hexarotor with $\gamma = 107^o$ and $\delta = 0^o$ for all motors, and a failure in M3, for the case of the random wind profile.

maximum value increases linearly with time. The direction of the perturbation changes every 5 seconds, and a low-pass filter is used in order to avoid sharp changes (which would represent unrealistic winds).

In Fig. 9, the attitude during the flight for the inwards vehicle with $\delta_1 = 0^o$ is shown. As long as the perturbations are small or in a not stressful direction (until $t = 15s$), the vehicle is able to hold position by performing adequate maneuvers, but after that moment the vehicle cannot exert the required torques, crashing at $t = 21s$. Also in the same figure, the corresponding PWM signals that drive the motors during the flight are presented. It is observed that M6 is the motor with the lowest speed, but that speed is still positive (even in the first 5 seconds). At $t = 16s$, the torque that needs to be exerted requires a negative speed from M6, which cannot be achieved.

In the same way, Fig. 10 shows the attitude for the vehicle with $\delta_1 = 10^o$, which is able to hold position during the full flight, and the corresponding PWM signals which are always within the limits, with M6 working at a higher speed, far away from saturation.

A second simulation was carried out with identical conditions as before, but this time considering a perturbation

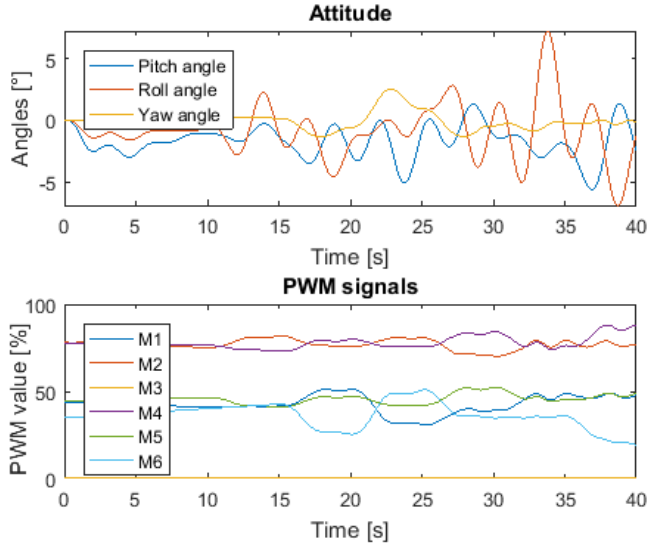

Fig. 10. Simulation results of the attitude and PWM signals of the inward-tilted hexarotor with $\gamma = 107^o$, $\delta_1 = 10^o$ and $\delta_i = 0^o$, $i = 2, ..., 6$, and a failure in M3, for the case of the random wind profile.

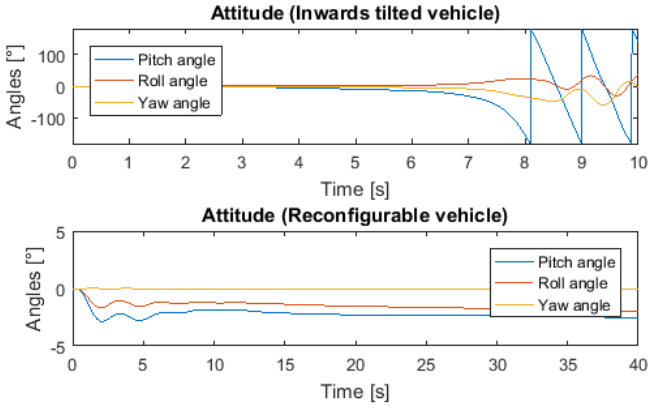

Fig. 11. Simulation results of the attitude of the inward-tilted hexarotor (top) and reconfigurable hexarotor (bottom), with a failure present in M3, for the case of the ramp wind profile.

torque that increases linearly with time according to $q_D = [-0.005, -0.01, -0.0005]t$. Its magnitude and direction were chosen so that the vehicle is forced to exert torque in a stressful direction. In Fig. 11, the attitude for both vehicles during the flight is shown. As the perturbation torque requires lowering the force exerted by M6 to counteract it, the inwards tilted vehicle is quickly destabilized, and crashes in less than 10s, while the proposed reconfigurable vehicle is able to hold the hovering state during the 40s of the simulation.

V. Experimental Setup

To provide experimental results, a setup used in previous experiments was adapted. The frame is the DJI-F550, with a distance between motors of 550mm. The actuators installed on this frame are T-Motor 2212-920KV motors, with 9545 plastic self-tightening propellers, driven by 20A electronic speed controllers (ESC). The battery used is a 4S 5000mAh 20C LiPo that allows approximately 15 minutes of hovering flight (without failures). The flight computer used is a custom-designed board [15] developed by the LAR-GPSIC Lab [16] to support experiments that are usually carried out on this kind of vehicles.

Several mechanical adapters were 3D-printed to achieve the tilted motor configuration. They provide an inward-tilting of $\gamma = 107^o$ for all motors, as shown in Fig. 1 (left). Another 3D-printed mechanism that allowed a servo to tilt the motor sideways was used for M1 (Fig. 1 (right)), while M3 was selected as the motor to present a failure.

The experiment consisted in the vehicle taking off with all motors working, setting the bias in the pitch and roll angles in order to achieve static hovering, activating a total failure in M3 through the remote control, recovering from the failure, and landing safely. The orientation of the vehicle during the full flight is shown in Fig. 12 (top). The vehicle takes off at $t = 3s$ and, due to the irregular ground effect produced by the propellers, is affected by several perturbations, until $t = 14s$, when it is flying at around $2m$ above the ground. At $t = 15.15s$, M3 is turned off, and the allocation matrix is changed from A to A_3, while maintaining the references for pitch and roll angles fixed. The vehicle recovers the hovering state at around $t = 18s$, and is then driven again to the take-off spot to land safely. A close-up of the moment of the failure is presented in Fig. 12 (middle), where it can be seen that the roll angle deviates around 7^o from its hovering position, and the pitch angle deviates only 5^o, as M3 has a low impact on the pitch control. From the moment of the occurrence of the failure, till $t = 20s$, the vehicle drifted around $2.5m$, time at which the pilot intervened.

Finally, in Fig. 12 (bottom), the PWM signals during the flight are presented. It is shown that all the signals operate in a similar range, between 50-70%, which gives plenty of room for speed variations in order to perform different maneuvers. This is an advantage with respect to previous works, in particular [8], where the slowest rotor presented a PWM signal of around 20%, while the PWM value at which the rotors turn on is around 15%, thus operating very close to the working limits. A video of one of the experimental flights performed can be found at [17].

In the previous experiment, the vehicle reconfigures at the same time that M3 is turned off, which does not represent a realistic case of failure, where the fault needs to be detected before the reconfiguration can take place. To get an idea of the behaviour of the vehicle in case of a delay in the detection and reconfiguration of the system, several experiments were carried out, where the fault is activated, and the system is reconfigured after a fixed time t_r, varying between $0ms$ and $400ms$ in steps of $100ms$. The attitude of the vehicle during these experiments is shown in Fig. 13, where the plots are adjusted so that the failure occurs at $t = 1s$. A video of this experiments can be found at [18].

Results show that with a delays of up to $400ms$ in the reconfiguration, the vehicle is able to recover to a hovering state. This indicates that the system would perform adequately when integrated with state-of-the-art fault-detection subsystems such as the bank of observers proposed in [2],

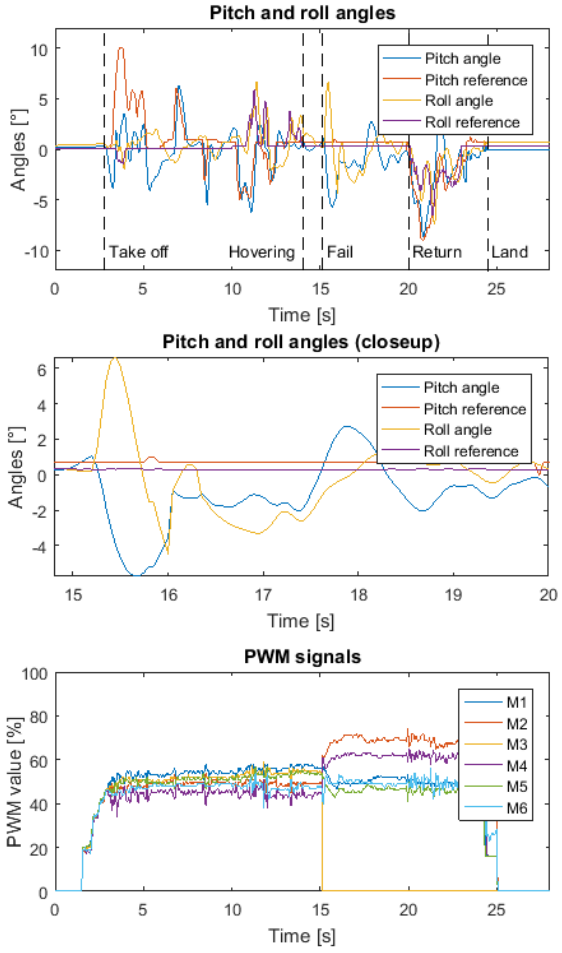

Fig. 12. Experimental flight of the inward-tilted hexarotor with $\gamma = 107^o$, and $\delta_i = 0^o,\ i = 2, ..., 6$. A failure occurs in rotor 3 at $t = 15.15s$, where δ_1 changes from 0^o to 10^o. The figures show the pitch and roll angles for the full flight (top), and for the moment for the failure (middle), as well as the PWM signals during the full flight (bottom).

[4], where detection and reconfiguration times below $400ms$ are reported.

Other experiments were carried out with a failure in M2 and M5 (tilting M1 according to Fig. 4) with good results and a similar behaviour to a failure in M3. A failure in M1, M4 or M6 would behave similarly to failures in M2, M3 or M5 (by tilting in this case M2), due to the symmetry of the vehicle.

VI. Conclusion

This article presented a numerical analysis and experimental results showing fault tolerance of a hexagon-shaped multirotor with a reconfigurable titled-rotor configuration. The proposed vehicle requires two additional servos, to reconfigure the rotors when the failure occurs.

The behaviour of the fault-tolerant vehicle is compared to previously proposed configurations, showing improvements on vehicle maneuverability when one of the rotors fails, for a hexarotor with similar characteristics to the vehicle used here, which is based on a commercial model. This does not mean that previous results are not capable of compensating

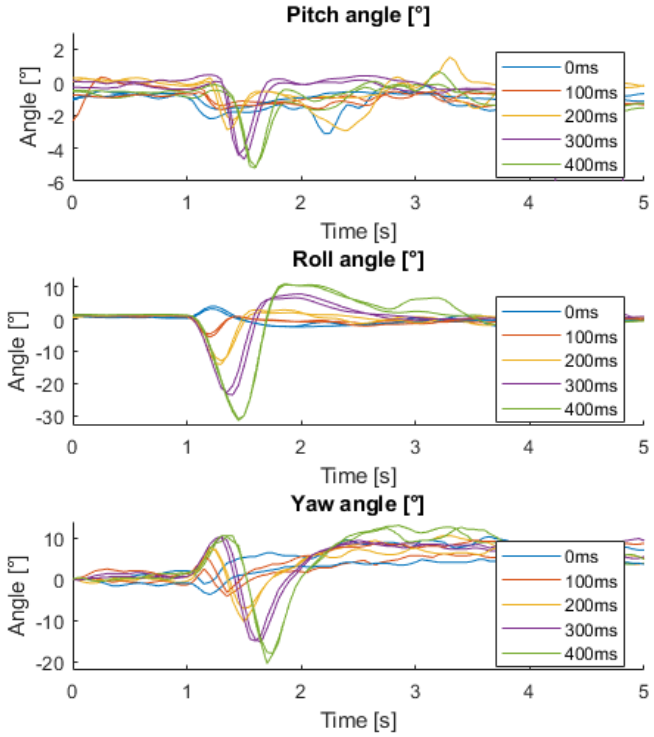

Fig. 13. Experimental flights showing the attitude of the inward-tilted hexarotor with $\gamma = 107^o$, and $\delta_i = 0^o,\ i = 2, ..., 6$. A failure occurs in rotor 3 at $t = 1s$, where δ_1 changes from 0^o to 10^o in $t = 1s + t_r$, for $t_r \in [0ms,\ 100ms,\ 200ms,\ 300ms,\ 400ms]$.

a failure, but in real scenarios, if a fail occurs mid-flight, this solution offers a wider range of applicable torques resulting in a more robust vehicle.

VII. Future work

A more exhaustive analysis of experimental results is being carried out, considering that a failure may occur during different vehicle maneuvers. Also, partial failures are being considered.

The focus of this work was on control allocation and not on the control algorithm used. Therefore, a PID controller was implemented to facilitate comparison with previous work. Exploring more advanced control methods may improve performance of the proposed system.

Experimental tests considering indoor trajectory following have been already performed for the vehicle with and without failure with satisfactory results [19], and also for an occurrence of the failure in the middle of the trajectory.

At the time of writing this work, experimental tests are being performed to evaluate a complete detection-and-reconfiguration system in an outdoor environment [20].

VIII. Acknowledgment

This work has been sponsored through the University of Buenos Aires, PDE2019, and Agencia Nacional de Promoción Científica y Tecnológica, FONCYT PICT 2016-2016 (2018-2020) (Argentina). Claudio Pose thanks the Peruilh foundation, whose grant made this research possible.

REFERENCES

[1] M. Saied, B. Lussier, I. Fantoni, C. Francis, H. Shraim, and G. Sanahuja, "Fault diagnosis and fault-tolerant control strategy for rotor failure in an octorotor," *IEEE International Conference on Robotics and Automation*, pp. 5266–5271, 2015.

[2] D. Vey and J. Lunze, "Structural reconfigurability analysis of multi-rotor UAVs after actuator failures," *54th Conference on Decision and Control*, pp. 5097–5104, 2015.

[3] D.-T. Nguyen, D. Saussie, and L. Saydy, "Fault-tolerant control of a hexacopter uav based on self-scheduled control allocation," in *2018 International Conference on Unmanned Aircraft Systems (ICUAS)*, 2018, pp. 385–393.

[4] D. Vey and J. Lunze, "Experimental evaluation of an active fault-tolerant control scheme for multirotor UAVs," *3rd International Conference on Control and Fault-Tolerant Systems*, pp. 119–126, 2016.

[5] G. P. Falcon, V. A. Marvakov, and F. Holzapfel, "Fault tolerant control for a hexarotor system using incremental backstepping," *IEEE Conference on Control Applications (CCA)*, pp. 237–242, 2016.

[6] M. W. Mueller and R. D'Andrea, "Stability and control of a quadrocopter despite the complete loss of one, two, or three propellers," in *2014 IEEE International Conference on Robotics and Automation (ICRA)*, May 2014, pp. 45–52.

[7] J. I. Giribet, R. S. Sanchez-Peña, and A. S. Ghersin, "Analysis and design of a tilted rotor hexacopter for fault tolerance," *IEEE Transactions on Aerospace and Electronic Systems*, vol. 52, no. 4, pp. 1555–1567, 2016.

[8] J. I. Giribet, C. D. Pose, A. S. Ghersin, and I. Mas, "Experimental validation of a fault tolerant hexacopter with tilted rotors," *International Journal of Electrical and Electronic Engineering and Telecommunications*, vol. 7, no. 2, pp. 1203–1218, 2018.

[9] G. Michieletto, M. Ryll, and A. Franchi, "Control of statically hoverable multi-rotor aerial vehicles and application to rotor-failure robustness for hexarotors," in *2017 IEEE International Conference on Robotics and Automation (ICRA)*, May 2017, pp. 2747–2752.

[10] M. Ryll, D. Bicego, and A. Franchi, "Modeling and control of fast-hex: A fully-actuated by synchronized-tilting hexarotor," in *2016 IEEE/RSJ International Conference on Intelligent Robots and Systems (IROS)*, Oct 2016, pp. 1689–1694.

[11] S. Rajappa, M. Ryll, H. H. Blthoff, and A. Franchi, "Modeling, control and design optimization for a fully-actuated hexarotor aerial vehicle with tilted propellers," in *2015 IEEE International Conference on Robotics and Automation (ICRA)*, May 2015, pp. 4006–4013.

[12] K. Bodie, Z. Taylor, M. Kamel, and R. Siegwart, "Towards efficient full pose omnidirectionality with overactuated mavs," *International Symposium of Experimental Robotics (ISER)*, 2018.

[13] M. Achtelik, K. M. Doth, D. Gurdan, and J. Stumpf, "Design of a multi rotor MAV with regard to efficiency, dynamics and redundancy," *AIAA Guidance, Navigation, and Control Conference*, 2012.

[14] "KST servo model DS215MG." [Online]. Available: https://www.kst-servos.com/app/download/19832534/DS215MG+V3.0+Datenblatt+.pdf

[15] L. Garberoglio, M. Meraviglia, C. D. Pose, J. I. Giribet, and I. Mas, "Choriboard III: A Small and Powerful Flight Controller for Autonomous Vehicles," in *2018 Argentine Conference on Automatic Control (AADECA)*, Nov 2018, pp. 1–6.

[16] "Grupo de Procesamiento de Señales, Identificación y Control." [Online]. Available: http://psic.fi.uba.ar

[17] "Fault tolerant control of a double-tilted hexacopter." [Online]. Available: https://www.youtube.com/watch?v=der3QUWz4Vg

[18] "Fault tolerant control under delays in the fault detection system." [Online]. Available: https://youtu.be/aEQJbIHgLGs

[19] C. D. Pose, F. Presenza, I. Mas, and J. I. Giribet, "Trajectory following with a MAV under rotor fault conditions," *11th International Micro Air Vehicle Competition and Conference (IMAV 2019)*, pp. 55–59, 2019.

[20] "Fault tolerant hexacopter - Outdoor flight test." [Online]. Available: https://www.youtube.com/watch?v=9CGn-OY6JQk